MOLECULAR AND CELLULAR BIOLOGY, June 1989, p. 2657–2664
0270-7306/89/062657-08$02.00/0

Vol. 9, No. 6

Multiple Proto-Oncogene Activations in Avian Leukosis Virus-Induced Lymphomas: Evidence for Stage-Specific Events

BRUCE E. CLURMAN† AND WILLIAM S. HAYWARD*

Sloan-Kettering Institute for Cancer Research, 1275 York Avenue, New York, New York 10021

Received 3 February 1989/Accepted 20 March 1989

We have examined avian leukosis virus-induced B-cell lymphomas for multiple, stage-specific oncogene activations. Three targets for viral integration were identified: c-*myb*, c-*myc*, and a newly identified locus termed c-*bic*. The c-*myb* and c-*myc* genes were associated with different lymphoma phenotypes. The c-*bic* locus was a target for integration in one class of lymphomas, usually in conjunction with c-*myc* activation. The data indicate that c-*myc* and c-*bic* may act synergistically during lymphomagenesis and that c-*bic* is involved in late stages of tumor progression.

Lymphoid leukosis, a B-cell lymphoma induced by avian leukosis viruses (ALVs), progresses through a series of clinically distinct stages (5, 19). The majority of ALV-induced lymphomas contain proviral integrations within or near the c-*myc* gene resulting in deregulated expression of c-*myc* (12). The insertional activation of c-*myc* appears to be an early event in lymphomagenesis (6, 20), but additional proto-oncogene activations may be required for progression to late stages of the disease.

Three stages have been identified in ALV-induced lymphoid leukosis (2, 5, 19). (i) The earliest detectable lesion is the transformed follicle, a hyperplastic bursal follicle in which the normal follicular architecture is obscured by an abnormal proliferation of lymphoblasts. The lymphoblasts, however, are confined to their follicle of origin during this early stage. As many as 100 transformed follicles may be present in a single bursa, but most of these regress during bursal involution. (ii) One (or occasionally more than one) of the transformed follicles gives rise to a bursal nodule (primary tumor), which is readily identifiable at necropsy. (iii) Tumor cells from the bursal nodule disseminate to other tissues, resulting in widespread metastases in liver, kidney, and spleen.

Recent observations in several experimental systems support the notion that c-*myc* activation alone is not sufficient to induce a fully malignant state. HB-1, a v-*myc*-containing virus, induces transformed follicles when virus-infected B cells are used to reconstitute a chemically ablated bursa (20, 34). Like ALV-induced transformed follicles, however, only a small proportion of these progress to become lymphomas, suggesting that additional genetic events may be required for late stages of tumor progression. Clonality has been observed in B-cell lymphomas induced by MC29 virus, an acute avian virus that carries a v-*myc* gene (13) and in murine monocytic tumors induced by a c-*myc*-containing retrovirus (3). In both cases, tumors would be expected to be nonclonal if *myc* alone were sufficient for tumor induction, because of the large number of target cells that would presumably be infected with the *myc*-containing viruses. One avian retrovirus, MH-2, carries both v-*myc* and a complementing oncogene, v-*mil* (11). In some T-cell leukemias induced by the nonacute murine leukemia viruses, c-*myc* and other candidate proto-oncogenes (e.g., *pim-1* and *pim-2*) have been found to be insertionally activated in the same tumor, suggesting a synergism between the different oncogenes (17, 28; A. Berns, personal communication; P. O'Donnell, personal communication).

Transgenic mice carrying a chimeric *myc* transgene linked to either a mouse mammary tumor virus enhancer (21, 32) or an immunoglobulin Cμ enhancer (1) develop a high incidence of mammary carcinoma or B-cell lymphoma, respectively. However, although a *myc* transgene is present in all cells and expressed in many different tissues, only a limited number of tumors develop after a long (and variable) latent period. Most important, the tumors are clonal, suggesting a requirement for an additional mutagenic event. The above in vivo observations are consistent with tissue culture experiments in which the activated *myc* gene demonstrates only limited ability to transform primary embryo fibroblasts, except when cells are cotransfected with a second cooperating oncogene (15, 26).

In this report we describe an experimental strategy to identify proto-oncogenes that might function (in cooperation with c-*myc*) to induce late stages of progression in ALV-induced B-cell lymphomas. The infection protocol, which was designed to facilitate both the occurrence and detection of multiple insertional activations, resulted in an exceptionally high incidence of lymphomas within an experimentally limited time period. Both c-*myc* and c-*myb* were found to be targets for insertional activation, although activation of each gene was associated with a different lymphoma phenotype. In addition, we have identified a new locus, termed c-*bic*, which was found to be a common target for integration in one class of lymphomas, most of which also carried insertionally activated c-*myc* genes.

MATERIALS AND METHODS

Viruses and chickens. Viral stocks of UR2AV′ (kindly provided by M. C. Simon) and RAV-2 were propagated in chicken embryo fibroblasts. Twelve-day embryos (gs^- chf^-; SPAFAS, Inc.) received 0.1 ml of UR2AV′ (10^5 to 10^6 PFU/ml) injected into a chorioallantoic vein. Birds receiving RAV-2 were injected intravenously with 0.2 ml of RAV-2 (10^5 to 10^6 PFU/ml). Birds were euthanized when they appeared very ill; all surviving birds were sacrificed at 16 weeks. Tissues for DNA and RNA extraction were flash frozen in liquid nitrogen and stored at −70°C. Tissue for histological analysis was preserved in phosphate-buffered

* Corresponding author.
† Present address: Brigham and Women's Hospital, Boston, MA 02115.

Formalin; histopathological examination was performed by H. Nguyen, Cornell University Medical College.

DNA extraction, restriction endonuclease digestion, and nucleic acid blot hybridization. High-molecular-weight DNA was prepared from frozen tissues as previously described (30). Genomic DNAs were digested for approximately 3 h with 2 to 5 U of restriction enzyme per μg of DNA, electrophoresed in 0.7% agarose gels in 1× Tris borate-EDTA buffer, transferred to Nytran membranes (Schleicher & Schuell, Inc.), and hybridized by the method of Southern (31). Filters were prehybridized for a minimum of 3 h in a solution containing 5× SSC (1× SSC is 0.15 M NaCl plus 0.015 M sodium citrate), 1× Denhardt, 0.5 mg of 4S RNA per ml, 0.5% sodium dodecyl sulfate, and 0.05 M sodium phosphate (pH 7.4) at 65°C, or at 37°C with the addition of 50% formamide, and hybridized overnight under the same conditions but with 5% dextran sulfate and 5×10^5 to 10×10^5 Cerenkov cpm of ^{32}P-labeled probe per ml of solution. Blots were washed twice for 15 min in 2× SSC–0.5% sodium dodecyl sulfate at room temperature, 30 min at 37°C, and 1 h at 65°C in 0.2× SSC–0.5% sodium dodecyl sulfate.

RNA purification and blot hybridization. Total RNA was prepared from frozen tissue, using the guanidinium isothiocyanate method as described by Maniatis et al. (16). One cycle of oligo(dT)-cellulose (Collaborative Research, Inc.) was used for poly(A)$^+$ RNA selection; glyoxalation, electrophoresis, and Northern (RNA) transfer were according to Maniatis et al. (16). Hybridization was at 65°C as described for DNA.

DNA probe preparation. High-specific-activity DNA probes (>5×10^8 Cerenkov cpm/μg of DNA) were prepared by incorporation of [α-^{32}P]dCTP (3,000 Ci/mmol; New England Nuclear Corp.) into DNA by the random priming method (7) using Klenow enzyme (Boehringer Mannheim Biochemicals) and random hexamers (Pharmacia).

The probes used were as follows. *myc* is a 900-base-pair *Eco*RI-*Hin*dIII fragment of the third exon of the chicken c-*myc* gene; *myb* is a *Bgl*I-*Eco*RI fragment of pMK1 (14); *env* is a 0.9-kilobase (kb) *Eco*RI-*Mst*II fragment of the *env* region from pUR2AV′ (29); *gag* is a 2.3-kb *Sac*I-*Eco*RI fragment of pRSV(SR-A); U5 is a 540-base-pair *Pvu*II fragment containing U5 and flanking plasmid sequences from pU5, a plasmid containing a 170-base-pair *Eco*RI-*Bst*EII fragment of the U5 region of RSV(SR-A); the chicken immunoglobulin light-chain probe is a 2.7-kb *Bam*HI-*Sal*I fragment of the (J+C) plasmid (24); and the *Mst*II *pol-env* probe is a 2.7-kb *Mst*II fragment of pUR2AV′ containing *env* and *pol* sequences. The oncogenes represented in the oncogene panel were *erbA*, *erbB*, c-*ets*, v-*ets*, v-*fps*, c-*mos*, Ha-*ras*, Ki-*ras*, N-*ras*, v-*rel*, v-*src*, v-*yes*, v-*abl*, *int-1*, v-*raf*, v-*mil*, *pim-1*, *pim-2*, v-*sis*, *met*, N-*myc*, c-*myc*, v-*fos*, v-*kit*, v-*ski*, *bcr*, v-*myb*, and *fms*.

Junction fragment cloning. Tumor DNAs were digested to completion with *Eco*RI and size fractionated on a 10 to 40% sucrose gradient (16). DNAs from appropriate fractions were ligated into *Eco*RI-digested, dephosphorylated lambda GT10 arms (Promega Biotec) and packaged by using Packagene extracts (Promega). The libraries were screened with U5 and/or *env* probes as described (4, 16). The insert of 415LNC was subcloned into pSP64 (Promega).

Cloning of c-*bic* cDNAs. RNA from tumor 465LN was double poly(A) selected and reverse transcribed by using a mixture of oligo(dT) and random hexamers and a Boehringer Mannheim cDNA synthesis kit. The cDNA was treated with additional RNase H, followed by T4 polI and Klenow. *Eco*RI linkers were added, and the cDNA was cloned into *Eco*RI-digested, dephosphorylated lambdaZAP arms (Stratagene) and packaged with GigaPack Gold extracts (Stratagene). The library was screened with the c-*bic* probe; positive clones were plaque purified and self-excised according to the protocols of the manufacturer.

TABLE 1. Tumor incidence in singly and doubly infected birds

Virus[a]	No. of birds with tumors/no. infected (%)[b]		
	Early lymphomas	Late lymphomas	Other
UR2AV′	0/27 (0)	6/27 (22)	0/27 (0)
RAV-2	0/25 (0)	0/25 (0)	0/25 (0)
UR2AV′ + RAV-2	5/30 (17)	20/30 (67)	9/30 (30)

[a] UR2AV′ was injected into 12-day embryos; RAV-2 was injected 7 days after hatching. All surviving birds were sacrificed at 16 weeks.

[b] Birds that died shortly after hatching (<4 weeks) of non-neoplastic disease or accidents are not included. Early lymphomas, Caused death at 5 to 7 weeks of age; late lymphomas, first observed at 3 months of age; other tumors, nephroblastomas and poorly differentiated sarcomas.

DNA sequence analysis. DNA sequence analysis of recombinant plasmids was performed by the dideoxy method (27) using synthetic oligonucleotides (17-mers) as primers. Double-stranded sequencing with Sequenase (U.S. Biochemicals) was performed according to the provided protocol, using 6% wedge gradient sequencing gels (International Biotechnologies Inc.).

RESULTS

Use of a double-infection protocol to study multiple insertional activations. The protocol used for these studies consisted of sequential infection of chickens with ALVs of two different subgroups. Twelve-day embryos were inoculated intravenously with UR2AV′, a subgroup A ALV. Sixteen days later (7 days after hatching), the birds were infected with RAV-2, a subgroup B ALV. The birds were observed for 4 months, at which time all survivors were sacrificed. Control groups received only a single infection, either the embryonic infection with UR2AV′ or RAV-2 alone at 7 days after hatching.

Two different subgroups of ALV were used to overcome the normal barrier to superinfection with virus of the same subgroup (interference), which is mediated by the viral *env* gene product (36). Cells infected with ALV are resistant to superinfection by viruses of the same subgroup but susceptible to other subgroups of ALV. The 16-day interval between infections was included to allow time for clonal expansion of cells that might have sustained an insertional activation of a proto-oncogene, such as c-*myc*, during the first round of infection. This expansion would produce an increased target cell population for rare insertional activations of second proto-oncogenes, presumably those that could complement cellular genes activated by the first infection. Because this protocol would greatly enhance the probability of a single cell sustaining multiple proto-oncogene activations, it should result in a higher incidence of neoplasia and/or a reduced latent period (if, as suggested above, activation of the second oncogene is the rate-limiting step). This prediction was confirmed in the experiments described below.

Double-infection protocol induced a high incidence of neoplasms. Approximately 83% (25/30) of the birds receiving both RAV-2 and UR2AV′ developed lymphomas (Table 1). Other neoplasms (nephroblastomas and angiosarcomas) also developed in 30% (9/30) of the birds. All of these tumors

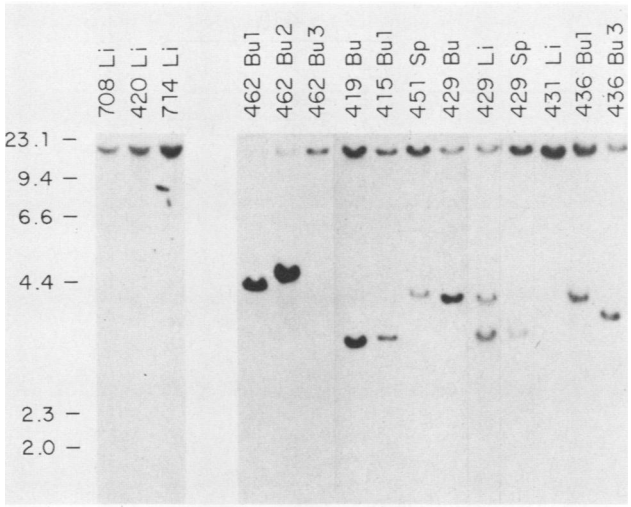

FIG. 1. Detection of c-*myc* rearrangements in lymphomas induced by double infection. Tumor DNAs were digested with *Eco*RI and hybridized to the c-*myc* probe. Samples include bursal nodules (Bu), liver (Li), and spleen (Sp) tumors. The first three tumors (708Li, 420Li, and 714Li) are early lymphomas; the remainder are late lymphomas. The 16-kb germ line *Eco*RI fragment is present in all samples. The smaller fragments are rearranged c-*myc* alleles.

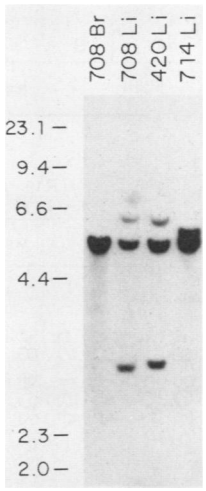

FIG. 2. Early lymphomas contained rearranged c-*myb* genes. *Eco*RI-digested DNA samples (Br, normal brain; Li, liver tumors) were hybridized with the c-*myb* probe. Three early lymphomas (708Li, 420Li, and 421Li) and a nonneoplastic control tissue (brain) are shown. The 5.5-kb germ line *Eco*RI fragment is present in all samples, including control tissue. Additional fragments in tumor samples are *myb* alleles rearranged by viral insertion.

occurred in birds also having lymphomas. Birds receiving only the first virus, UR2AV′, developed lymphomas at a much lower frequency, 22% (6/27), and no other tumors were found in this group. None of the birds receiving only RAV-2 at 7 days after hatching showed any signs of neoplastic disease during the 4-month period.

The lymphomas in birds receiving both viruses fell into two distinct classes, early and late, based on the latent period and clinical presentation. Early lymphomas caused death within 5 to 7 weeks after hatching and presented with widespread metastases in the absence of discrete bursal nodules. These tumors were of B-cell origin, as indicated by the presence of rearrangements in the immunoglobulin lambda locus and expression of immunoglobulin lambda mRNA. Late lymphomas were first detected at about 3 months after hatching, although the majority were found only after the birds were sacrificed at 4 months. The late lymphomas exhibited classic features of lymphoid leukosis, including extensive bursal involvement.

Early lymphomas occurred in 17% (5/30) of the doubly infected birds (Table 1). No early lymphomas were found in birds receiving UR2AV′ alone. Late lymphomas occurred in 67% (20/30) of the doubly infected birds and in 22% (6/27) of the birds infected only with UR2AV′.

Late lymphomas contained viral integrations within the c-*myc* gene. Because the c-*myc* gene is frequently a target for insertional activation in ALV-induced lymphomas, we screened lymphoma DNAs for c-*myc* rearrangements. Approximately 70% (24/34) of the late lymphomas exhibited tumor-specific c-*myc* rearrangements (Fig. 1). No c-*myc* rearrangements were found in early lymphomas (0/4). At necropsy, most of the birds with late lymphomas were found to have multiple bursal nodules and variable metastatic disease. In most cases, individual bursal nodules from a single bird had different *myc* rearrangements and thus appeared to be composed of clonally independent cell populations (e.g., birds 436 and 462, Fig. 1). The 34 late lymphomas surveyed were obtained from 16 different birds.

Early lymphomas contained viral integrations within the c-*myb* gene. Our laboratory has recently found that the chicken c-*myb* gene is a target for insertional activation in lymphomas induced by EU-8 virus (14), a recombinant ALV constructed by inserting the UR2AV′ *env* gene into the genome of ringnecked pheasant virus (29). The early lymphomas induced with the double-infection protocol resembled the EU-8-induced lymphomas in the following ways: (i) short latent period (5 to 8 weeks), (ii) absence of extensive bursal involvement, and (iii) absence of c-*myc* rearrangements.

All of the early lymphomas tested (4/4) contained c-*myb* rearrangements (Fig. 2). Integrations fell within the same upstream region of c-*myb* that was the major target in EU-8-induced early lymphomas. Thus, both biologically and at the molecular level, these tumors were indistinguishable from the EU-8 induced lymphomas. No c-*myb* rearrangements were found in any of the late lymphomas tested (0/28).

Identification of virus-specific internal fragments and virus-cell junction fragments. The strains of subgroup A and B ALV used in these studies were chosen because they each contain unique diagnostic restriction sites. An *Mst*II fragment of UR2AV′, containing *pol* and *env* sequences, was used to probe *Eco*RI-digested DNAs. The probe detects UR2AV′ internal fragments of 2.2 and 1.7 kb and RAV-2 internal fragments of 3.8 and 1.3 kb (Fig. 3).

An analysis of DNAs from three early lymphomas (420Li, 421Li, and 708Li) and a late lymphoma (451Sp), all from doubly infected birds, and a late lymphoma from a bird that received only UR2AV′ (204Li) is shown in Fig. 3. DNAs from nonneoplastic control tissue (brain) from several birds are also included. The diagnostic UR2AV′ internal fragments were present in all of the samples; thus, all of these tissues (including normal brain from infected birds) were infected with this virus. Because the RAV-2 "A" fragment comigrated with an *Eco*RI fragment present in endogenous proviruses, only the RAV-2 "B" fragment was useful diagnostically. This fragment was present in all of the tissues from doubly infected birds, although the levels were lower in control tissues than in tumors. As expected, the RAV-2 "B"

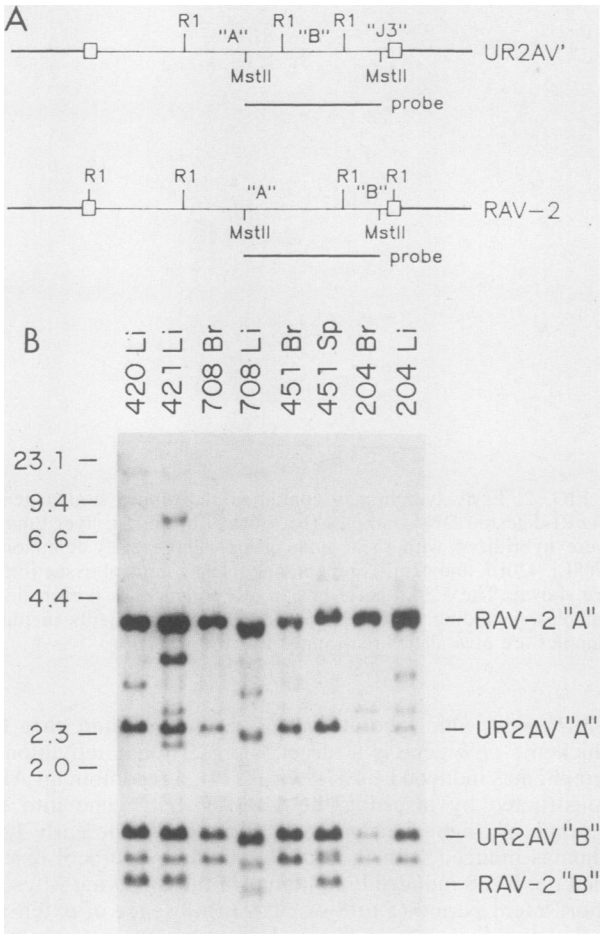

FIG. 3. Detection of virus-specific internal fragments in tumors induced by double infection. (A) *Eco*RI restriction maps of UR2AV′ and RAV-2 indicating the two internal fragments of each virus ("A" and "B") that are detected by the *pol-env* probe (see text). "J3" indicates the 3′ UR2AV′-cell junction fragment which is also detected by the probe. (B) *Eco*RI-digested DNAs (Li, liver tumors; Br, normal brain; Sp, spleen tumors) were hybridized to the *pol-env* probe. Bands corresponding to internal fragments of each virus are indicated. Other bands represent either endogenous viruses (in both normal and tumor tissue) or tumor-specific UR2AV′ junction fragments. Samples include three early lymphomas (420Li, 421Li, 708Li), a late lymphoma (451Sp), a lymphoma induced by infection with only UR2AV′ (204Li), and nonneoplastic control tissues (Br). Sizes are shown in kilobases on the left.

fragment was not present in tissues from bird 204, which was infected only with UR2AV′. Nearly all of the tumors from doubly infected birds were analyzed in this way, and all of these (both early and late tumors) were found to be infected with both viruses.

Clonal integrations of each virus can also be distinguished with a similar strategy to characterize virus-host junction fragments. After *Eco*RI digestion, the 3′ virus-host junction fragments of UR2AV′ hybridize with both *env* and U5 probes; those from RAV-2 hybridize only with the U5 probe (Fig. 3A). An analysis of 20 late lymphoma DNAs showed that all of the rearranged c-*myc* genes were associated with integrated proviruses; 60% (12/20) of these were UR2AV′, and 40% (8/20) were RAV-2 (data not shown). A similar examination of the early lymphoma DNAs demonstrated that all of the c-*myb*-associated proviruses were UR2AV′.

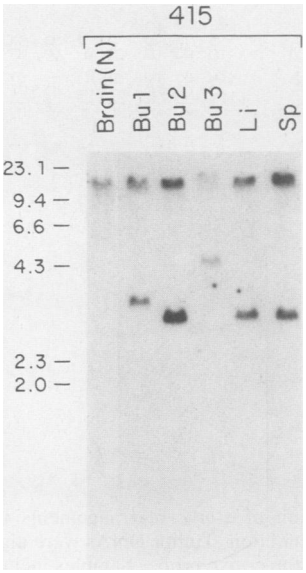

FIG. 4. Three independent *myc*-rearranged cell populations in bird 415. *Eco*RI-digested DNAs (Bu, bursal nodule; Li, liver tumor; Sp, spleen tumor) from various tissues from bird 415 were hybridized to the *myc* probe. The 16-kb germ line c-*myc* band is present in all samples. Each bursal nodule (Bu1, Bu2, and Bu3) contained a different rearrangement in c-*myc*. The rearranged c-*myc* genes in the two metastatic tumors (Li and Sp) corresponded to that found in Bu2. Normal brain (N) DNA was used as a control. Sizes are shown in kilobases on the left.

Identification and characterization of a candidate *myc*-complementing oncogene. The search for candidate oncogenes was performed by screening late lymphoma DNAs for integration sites other than c-*myc* that were common to independently derived tumors. Probes for this purpose were derived from three different junction fragments cloned from a liver tumor in bird 415.

Bird 415 contained three independent bursal nodules (primary tumors) plus metastatic tumors in liver and spleen. All of the tumors from this bird contained c-*myc* rearrangements (Fig. 4). Each of the three bursal nodules had *myc Eco*RI fragments of a different length (3.6, 3.4, and 4.3 kb); thus, each represented a distinct clonal population arising from an independent c-*myc* integration. The metastatic tumors (liver and spleen nodules [Fig. 4] and a diffuse liver tumor [not shown]) displayed rearranged c-*myc* fragments of 3.4 kb that comigrated with the fragment from bursal nodule 2, suggesting that they were derived from bursal nodule 2. Although all three bursal nodules were similar in size and appearance, it appeared that only bursal nodule 2 had acquired the ability to metastasize.

DNAs from bursal nodule 2 and the metastatic nodules were further analyzed to identify tumor-specific junction fragments that might represent insertionally activated *myc*-complementing loci. When hybridized with the U5 probe, each of the tumor DNAs was found to contain at least three U5$^+$ tumor-specific junction fragments, in addition to the *myc*-associated junction fragment (3.4 kb) (Fig. 5A). DNAs from the liver nodule, spleen nodule (not shown), and bursal nodule 2 also contained a 7.5-kb *env*-specific junction fragment that was not present in DNAs from bursal nodules 1 and 3 or from control tissue (Fig. 5B). (This provirus had apparently sustained a deletion at its 3′ end, because the

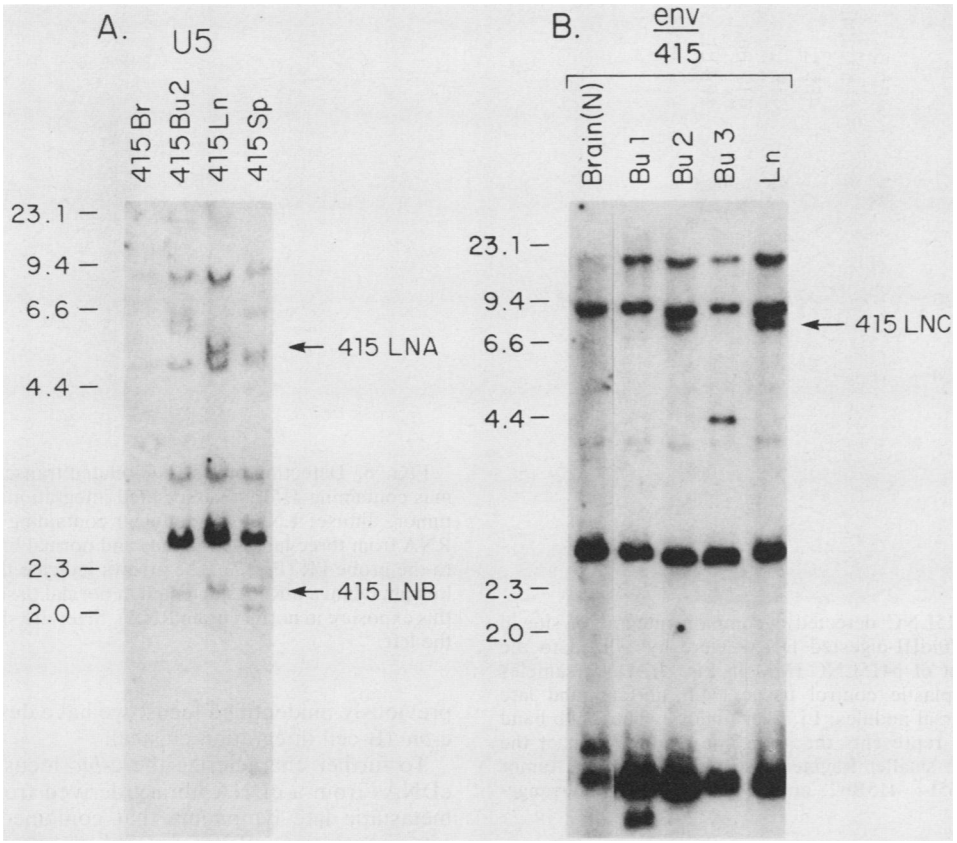

FIG. 5. Detection of tumor-specific junction fragments in lymphomas from bird 415. *Eco*RI-digested DNAs (Br, normal brain; Bu, bursal nodule; Ln, liver nodule; Sp, spleen tumor) were hybridized to either the U5 (A) or *env* (B) probes. Multiple tumor-specific integrations were observed in each sample. The arrows indicate the three junction fragments (LNA, LNB, and LNC) that were cloned from the liver nodule. Additional bands present in both tumor and control (Br) samples represent endogenous proviruses and internal viral fragments. Sizes are shown in kilobases on the left of the panels.

junction fragment was detected with *env* probe but not with U5 probe.)

All of the tumor-specific junction fragments (except the 3.4-kb *myc*-associated fragment) from a single metastatic tumor, 415Ln, were cloned: the 5.3-kb $U5^+$ fragment, which is unique to this tumor, and the 2.1 kb $U5^+$ and the 7.5-kb env^+ fragments common to bursal nodule 2 and the metastatic tumors (Fig. 5, 415LNA, 415LNB, and 415LNC, respectively). Restriction fragments free of viral sequences were generated from each cloned junction fragment and used as probes to screen late lymphoma DNAs.

Neither the 415LNA nor the 415LNB probes detected rearrangements in any tumors except those from bird 415 (data not shown). Clone 415LNC, however, was found to represent an integration site that was common to many different lymphomas. The 415LNC probe hybridized to a 23-kb germ line *Hin*dIII fragment present in DNA from all tissues, including normal muscle (465Mu), but also hybridized to smaller fragments in DNA from 415 bursal nodule 2 and from several other independent tumors (Fig. 6). An analysis of 34 late lymphoma DNAs revealed 415LNC rearrangements in 10 tumors, 8 of which were clonally independent. The locations of seven independent integrations within the 415LNC locus are shown in Fig. 7. All of these integrations were in the same transcriptional orientation. Because of extensive viral deletions and recombination events, the 415LNC-associated proviruses could not be identified with certainty as either UR2AV′ or RAV-2. No rearrangements within the 415LNC locus were found in any of the early lymphomas (0/4). Likewise, no rearrangements in this locus were found in a series of EU-8-induced early lymphomas (0/8).

Clone 415LNC detected altered mRNAs in tumors with integrations within the 415LNC locus. To determine if viral insertions within the 415LNC locus result in transcription of adjacent cellular sequences, restriction fragments of the 415LNC clone were used to probe Northern blots containing poly(A)$^+$ RNA from late lymphomas and normal tissues. The 3-kb *Mst*II fragment (Fig. 7, probe MM) did not detect mRNA in any tissue examined. However, a 1.5-kb *Pvu*II-*Eco*RI fragment (probe PR) detected very abundant transcripts in several tumors with viral insertions in this region (Fig. 8). The transcripts were very heterogeneous in size, and the patterns for each of the tumors were different. The significance of any particular transcript is thus uncertain, but it is clear that integrations within this locus resulted in high expression of tumor-specific mRNAs.

415LNC-homologous RNA was either undetectable or present at barely detectable levels in normal tissues (bursa, thymus, kidney, liver, and brain) from uninfected birds. Among the tissues tested, the highest level of expression was found in the brain, which contained low-abundance transcripts of about 4 kb (Fig. 8, arrows). These data support the notion that the DNA sequence represented by the 415LNC clone is a cellular gene that is insertionally activated in late lymphomas.

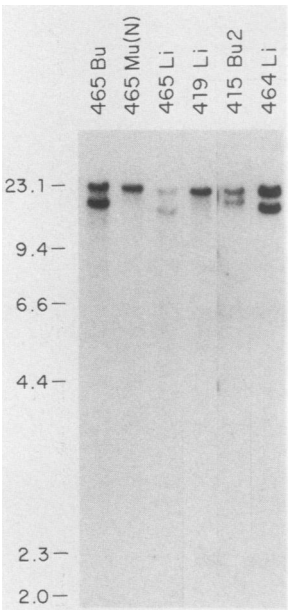

FIG. 6. Clone 415LNC detected a common integration site in late lymphomas. *Hin*dIII-digested DNAs were hybridized to the 3-kb *Mst*II fragment of p415LNC (MM in Fig. 7). DNA samples were from nonneoplastic control tissue (Mu, muscle) and late lymphomas (Bu, bursal nodules; Li, liver tumors). The 23-kb band present in all lanes represents the germ line configuration of the 415LNC locus. The smaller fragments seen in four of the tumor samples (465Bu, 465Li, 415Bu2, and 464Li) represent rearrangements of the locus.

Characterization of the 415LNC locus. In an effort to determine whether the 415LNC clone represents a previously identified proto-oncogene, we hybridized the *Pvu*II-*Eco*RI fragment (Fig. 7, probe PR) to a panel of DNA clones representing 28 known oncogenes (see Materials and Methods). The probe failed to hybridize to any of these oncogene DNAs (data not shown). We therefore sequenced approximately 2 kb of 415LNC surrounding the region that detected mRNAs (probe PR). Comparison of this sequence (in both orientations) with sequences in the GenBank data base, using the FASTN program, revealed no significant homologies. Furthermore, the predicted amino acid sequences of all three reading frames in both orientations showed no significant homology with sequences in the Dayhoff and Doolittle protein data bases. Since 415LNC appears to represent a

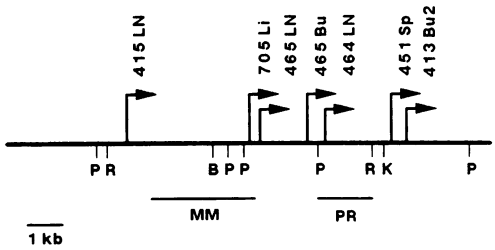

FIG. 7. Restriction map of the 415LNC (c-*bic*) locus and distribution of proviral integrations. Arrows show the locations and orientations of proviruses integrated within the 415LNC locus in seven independent late lymphomas. Sequences corresponding to the MM probe (a 3-kb *Mst*II-*Mst*II fragment) and the PR probe (a 1.5-kb *Pvu*II-*Eco*RI fragment) are indicated below the map. Restriction sites: B, *Bgl*I; K, *Kpn*I; P, *Pvu*II; R, *Eco*RI.

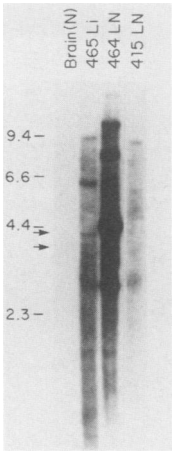

FIG. 8. Detection of 415LNC-related transcripts in late lymphomas containing 415LNC-associated integrations. Samples (Li, liver tumor, diffuse; LN, liver nodules) containing 2.5 μg of poly(A)$^+$ RNA from three late lymphomas and normal brain were hybridized to the probe PR (Fig. 7). The arrows indicate the band positions of low-abundance mRNAs detected in normal tissues (barely visible at this exposure in normal brain RNA). Sizes are shown in kilobases on the left.

previously unidentified locus, we have designated this locus c-*bic* (B-cell integration cluster).

To further characterize the c-*bic* locus, we cloned c-*bic* cDNAs from a cDNA library derived from tumor 465Li, a metastatic late lymphoma that contained both c-*myc* and c-*bic* integrations. Several cDNA clones were obtained, and a 4.4-kb cDNA designated pbicB1A was selected for further analysis. The pbicB1A cDNA did not hybridize to any of the 28 oncogene DNAs. However, it did hybridize to both c-*bic* and ALV probes. Sequence analyses of the termini of the cDNA clone confirmed that it contained both c-*bic* and viral (*pol* gene) sequences. This structure suggests that the RNA from which the cDNA clone was derived resulted from transcription initiating within the proviral DNA and reading into the adjacent *bic* DNA sequences. However, because of the complex pattern of c-*bic* transcripts in this tumor, the biological significance of this and other tumor-specific *bic* transcripts must await further investigation.

DISCUSSION

Double infection resulted in enhanced tumorigenesis. The double-infection protocol was designed to facilitate superinfection of infected cells that had sustained an insertional activation, thus increasing the probability that more than one proto-oncogene would be insertionally activated in the same clonal cell population. As predicted, birds infected with both UR2AV′ at day 12 of embryogenesis and RAV-2 at 7 days after hatching had a much higher incidence of lymphoma at 16 weeks (83%) than those receiving only the embryonic infection (22%) or the 7-day infection (0%). In addition, an unusually high proportion of these birds had multiple, clonally independent tumors.

The lymphomas fell into two discrete classes, early and late, based on latency. Although both were B-cell lymphomas, they were biologically and molecularly distinct. The early lymphomas induced with the double-infection protocol were identical in all properties tested to those induced by EU-8 virus (14, 29). The late lymphomas were indistinguishable from classic lymphoid leukosis induced by a single ALV

TABLE 2. Proto-oncogene activations in early and late lymphomas

Locus	Early lymphomas	Late lymphomas	
		Primary	Metastatic
c-*myb*	4/4 (100)	0/21 (0)	0/12 (0)
c-*myc*	0/4 (0)	14/21 (67)	9/12 (75)
c-*bic*	0/4 (0)	3/21 (14)	6/12 (50)

infection, except that the latent period was reduced by at least 1 month with the double-infection protocol and the average number of clonal integrations per tumor was significantly higher. All of the double-infection-induced late lymphomas contained at least two clonal integrations, and tumors with five or more integrations were common.

Three common integration sites were identified in lymphomas induced by double infection: c-*myb*, c-*myc*, and c-*bic*. Integrations within c-*myb* occurred only in early lymphomas, whereas integrations within c-*myc* and c-*bic* were found only in late lymphomas.

Activation of both c-*myc* and c-*bic* in late lymphomas. Although integrations within c-*myb* and c-*myc* were mutually exclusive events, integrations within c-*myc* and c-*bic* were often found in the same tumor. Activation of these two loci may thus provide transforming activities that act synergistically during the progression of late lymphomas. Interestingly, most of the c-*bic* integrations were found in metastatic tumors. While the frequencies of c-*myc* integrations (approximately 70%) were similar in both primary tumors and metastatic tumors, the frequency of c-*bic* integrations was higher in metastases (50%) than in primary tumors (14%) (Table 2). These data suggest a model for tumor progression in which the activation of c-*myc* is an early event in lymphomagenesis and activation of c-*bic* is a late event, possibly involved in metastasis. This model is consistent with the observations that the vast majority of transformed follicles in lymphoid leukosis contain insertionally activated c-*myc* genes (6) and that most transformed follicles do not progress to form tumors (2, 20, 34).

Insertional activation of c-*bic* might be expected to occur less frequently in lymphomas induced by infection with a single ALV because superinfection would be blocked by interference. Many of those lymphomas do contain more than one integrated provirus (9, 18, 23) however, perhaps as a consequence of deletions in c-*myc*-associated proviruses, which abolish *env* expression (8–10, 18, 22, 23, 25, 33). A screening of lymphoma DNAs from earlier studies (10, 12, 18) in which lymphoid leukosis was induced by single infection with RAV-1 or RAV-2 revealed c-*bic* rearrangements in 2 of 14 (15%) of the tumors (data not shown). Both of these tumors also contained *myc* integrations and were metastatic.

Although *bic* and *myc* are involved in a high proportion of metastatic lymphomas, the existence of tumors with viral integrations within only one, or neither, of these loci suggests that there are other cellular genes that can substitute for these loci and provide similar functions. However, our estimates for the involvement of these two loci may be low because of the limitations of the assay used. Rearrangements could only be detected within the regions accessible to restriction analysis with the available probes, and minimal rearrangements or single base changes would not have been detected.

The sequence analysis of the *bic* genomic DNA and cDNA clones and the lack of hybridization of these clones with DNAs of known oncogenes support the identification of c-*bic* as a novel locus. The *bic* probe detected low-abundance transcripts in several normal tissues, and heterogeneous, highly expressed mRNAs in late lymphomas carrying c-*bic* rearrangements. The presence of these transcripts suggests that integrations within this locus result in insertional activation of a resident cellular gene.

Determinants of early and late lymphomagenesis. The target cell for classic lymphoid leukosis is thought to be a bursal stem cell, which arises during embryogenesis and persists for several weeks after hatching (34, 35). The target for early lymphomas, however, may be a prebursal stem cell which is present only in the embryo. All of the c-*myc*-associated proviruses in the double-infection-induced early lymphomas resulted from the embryonic infection (i.e., UR2AV'). Furthermore EU-8 virus, which induces a high incidence of early lymphomas when injected into the embryo, induces only c-*myc*-associated late lymphomas when injected after hatching (14; M. Kanter, R. E. Smith, and W. S. Hayward, unpublished data). These observations suggest that the target cell for early lymphomas is no longer present after hatching, whereas bursal stem cells are still present at this time. The distinct biological characteristics of the early and late lymphomas may thus reflect properties of both the target cells and proto-oncogenes involved.

Early lymphomas generally had fewer integrations than did the late lymphomas. One of the early lymphomas analyzed in this study had only a single clonal integration (within c-*myb*), and approximately 50% of the more than 20 EU-8-induced early lymphomas analyzed previously had only c-*myb*-associated integrations (14). Thus, activation of c-*myb* alone may be sufficient to induce early lymphoma. The role of the second virus (RAV-2) in the induction of early lymphoma is currently unknown. Both the short latency and the biology of this disease (which does not appear to pass through the transformed follicle and bursal nodule stages characteristic of late lymphoma) support a single-step model for early lymphoma. In contrast, at least two activated proto-oncogenes, c-*myc* and c-*bic*, have been implicated in late lymphoma, and involvement of additional oncogenes must also be considered. The difference in latent periods for early and late lymphoma could thus reflect the time required to accumulate multiple proto-oncogene activations in the long-latency disease.

ACKNOWLEDGMENTS

We thank George Vande Woude, Karen Beemon, and Madge Kanter for critical reading of the manuscript; Anton Berns, Paul O'Donnell, Don Ewert for communicating unpublished data; and our many colleagues who provided oncogene probes. We also thank Nancy Heyman for expert technical assistance.

Work in our laboratory was supported by Public Health Service grants CA-43250 and CA-16599 from the National Institutes of Health. B.E.C. is a Rudin Fellow in the Medical Scientist Training Program of the Sloan-Kettering Institute and Cornell University Medical College.

LITERATURE CITED

1. **Adams, J. M., A. W. Harris, C. A. Pinkert, L. M. Corcoran, W. S. Alexander, R. D. Palmiter, and R. L. Brinster.** 1985. The c-*myc* oncogene driven by immunoglobulin enhancers induces lymphoid malignancy in transgenic mice. Nature (London) **318**:533–538.
2. **Baba, T., and E. H. Humphries.** 1985. Formation of a transformed follicle is necessary but not sufficient for development of

an avian leukosis virus-induced lymphoma. Proc. Natl. Acad. Sci. USA **82**:213–216.
3. **Baumbach, W. R., E. J. Keath, and M. D. Cole.** 1986. A mouse c-*myc* retrovirus transforms established fibroblast lines in vitro and induces monocyte-macrophage tumors in vivo. J. Virol. **59**:276–283.
4. **Benton, W. D., and R. W. Davis.** 1977. Screening for lambda gt recombinant clones by hybridization to single plaques *in situ*. Science **196**:180–182.
5. **Cooper, M. D., L. E. Payne, P. B. Dent, B. P. Burmester, and R. A. Good.** 1968. Pathogenesis of avian lymphoid leukosis. J. Natl. Cancer Inst. **41**:374–389.
6. **Ewert, D. L., and G. F. DeBoer.** 1988. Avian lymphoid leukosis: mechanism of lymphomoganesis. Adv. Vet. Sci. Comp. Med. **32**:37–55.
7. **Feinberg, A. P., and B. Vegelstein.** 1983. A technique for radiolabeling DNA restriction fragments to high specific activity. Ann. Biochem. **132**:6–13.
8. **Fung, Y.-K., L. B. Crittenden, and H.-J. Kung.** 1982. Orientation and position of avian leukosis virus DNA relative to the cellular oncogene c-*myc* in B-lymphoma tumors of highly susceptible $15I_5X7_2$ chickens. J. Virol. **44**:742–746.
9. **Fung, Y.-K., A. M. Fadley, L. B. Crittenden, and H.-J. Kung.** 1981. On the mechanism of retrovirus-induced avian lymphoid leukosis: deletion and integration of the provirus. Proc. Natl. Acad. Sci. USA **78**:3418–3422.
10. **Goodenow, M. M., and W. S. Hayward.** 1987. 5′ Long terminal repeats of *myc*-associated proviruses appear structurally intact but are functionally impaired in tumors induced by avian leukosis viruses. J. Virol. **61**:2489–2498.
11. **Graf, T., F. V. Weizsaecker, S. Grieser, J. Coll, D. Stehelin, T. Patschinsky, K. Kister, C. Bechade, G. Calothy, and A. Leutz.** 1986. v-*mil* induced autocrine growth and enhanced tumorigenicity in v-*myc*-transformed avian macrophages. Cell **45**:357–364.
12. **Hayward, W. S., B. G. Neel, and S. M. Astrin.** 1981. Activation of a cellular oncogene by promoter insertion in ALV-induced lymphoid leukosis. Nature (London) **290**:475–480.
13. **Hayward, W. S., C.-K. Shih, and C. Moscovici.** 1983. Induction of bursal lymphomas by myelocytomatosis virus-29 (MC29). UCLA Symp. Mol. Cell. Biol. **5**:279–287.
14. **Kanter, M. R., R. E. Smith, and W. S. Hayward.** 1988. Rapid induction of B-cell lymphomas by EU-8 virus: insertional activation of the c-*myb* genes. J. Virol. **62**:1423–1432.
15. **Land, H., L. Parada, and R. A. Weinberg.** 1983. Tumorigenic conversion of primary embryo fibroblasts requires at least two cooperating oncogenes. Nature (London) **304**:296–602.
16. **Maniatis, T., E. F. Fritsch, and J. Sambrook.** 1982. Molecular cloning: a laboratory manual. Cold Spring Harbor Laboratory, Cold Spring Harbor, N.Y.
17. **Mucenski, M. L., D. J. Gilbert, B. A. Taylor, N. A. Jenkins, and N. G. Copeland.** 1987. Common sites of viral integration in lymphomas arising in AKXD recombinant inbred mouse strains. Oncogene Res. **2**:33–48.
18. **Neel, B. G., W. S. Hayward, W. L. Robinson, J. Fang, and S. M. Astrin.** 1981. Avian leukosis virus-induced tumors have common proviral integration sites and synthesize discrete new RNAs: oncogenesis by promoter insertion. Cell **23**:323–334.
19. **Neiman, P. E., L. Jordan, R. A. Weiss, and L. N. Payne.** 1980. *In* M. Essex, G. Todaro, and H. Zurhausen (ed.), Viruses in naturally occurring cancers, book A. Cold Spring Harbor Laboratory, Cold Spring Harbor, N.Y.
20. **Neiman, P. E., C. Wolf, P. J. Enrietto, and G. M. Cooper.** 1985. A retroviral *myc* gene induces preneoplastic transformations of lymphocytes in a bursal transplantation assay. Proc. Natl. Acad. Sci. USA **82**:222–226.
21. **Pattengale, P., P. Leder, A. Kuo, and T. Stewart.** 1986. Lymphohemopoietic and other neoplasms occurring spontaneously in transgenic mice carrying and expressing MTV/*myc* fusion genes. Curr. Top. Microbiol. Immunol. **132**:9–16.
22. **Payne, G. S., J. M. Bishop, and H. Varmus.** 1982. Multiple arrangements of viral DNA and an activated host oncogene in bursal lymphomas. Nature (London) **295**:209–214.
23. **Payne, G. S., S. A. Courtneidge, L. B. Crittenden, A. M. Fadley, J. M. Bishop, and H. E. Varmus.** 1981. Analysis of avian leukosis virus DNA and RNA in bursal tumors: viral gene expression is not required for maintenance of the tumor state. Cell **23**:311–322.
24. **Reynaud, C.-A., V. Anquez, A. Dahan, and J.-C. Weill.** 1985. A single rearrangement event generates most of the chicken immunoglobulin light chain diversity. Cell **40**:283–291.
25. **Robinson, H. L., and G. C. Gagnon.** 1986. Patterns of proviral insertion and deletion in avian leukosis virus-induced lymphomas. J. Virol. **57**:28–36.
26. **Ruley, H. E.** 1983. Adenovirus early region 1A enables viral and cellular genes to transform primary cells in culture. Nature (London) **304**:602–606.
27. **Sanger, F., S. Nicklen, and A. R. Coulson.** 1977. DNA sequencing with chain-terminating inhibitors. Proc. Natl. Acad. Sci. USA **74**:5463–5467.
28. **Selten, G. H., M. Cuypers, and A. Berns.** 1985. Proviral activation of the putative oncogene *pim*-1 in MuLV induced T-cell lymphomas. EMBO J. **4**:1793–1798.
29. **Simon, M. C., W. S. Neckameier, W. S. Hayward, and R. E. Smith.** 1987. Genetic determinants of neoplastic diseases induced by a subgroup F avian leukosis virus. J. Virol. **61**: 1203–1212.
30. **Simon, M. C., R. E. Smith, and W. S. Hayward.** 1984. Mechanisms of oncogenesis by subgroup F avian leukosis virus. J. Virol. **52**:1–8.
31. **Southern, E. M.** 1975. Detection of specific sequences among DNA fragments separated by gel electrophoresis. J. Mol. Biol. **98**:503–517.
32. **Stewart, T. A., P. K. Pattengale, and P. Leder.** 1985. Spontaneous mammary adenocarcinomas in transgenic mice that carry and express MTV/*myc* fusion genes. Cell **38**:627–637.
33. **Swift, R. A., N. Boerkoel, A. Ridgeway, D. Fujitsu, J. Dodgson, and H.-J. Kung.** 1987. B-lymphoma induction by reticuloendotheliosis virus: characterization of a mutated chicken syncytial virus provirus involved in c-*myc* activation. J. Virol. **610**: 2084–2090.
34. **Thompson, C. B., E. H. Humphries, L. M. Carlson, C.-L. Chen, and P. E. Neiman.** 1987. The effect of alterations in *myc* gene expression on B-cell development in the bursa of Fabricius. Cell **51**:371–378.

34a. **Tsichlis, P. N., P. G. Strauss, and M. A. Lohse.** 1985. Concerted DNA rearrangements in Moloney murine leukemia virus-induced thymomas: a potential synergistic relationship in oncogenesis. J. Virol. **56**:258–267.

35. **Weill, J.-C., M. Leibowitch, and C. A. Reynaud.** 1987. Questioning the role of the embryonic bursa in the differentiation of B lymphocytes. Curr. Top. Microbiol. Immunol. **135**:111–124.
36. **Weiss, R.** 1982. Experimental biology and assay of RNA tumor viruses, p. 209–260. *In* R. Weiss, N. Teich, H. Varmus, and J. Coffin (ed.), RNA tumor viruses, vol. 1. 2nd ed. Cold Spring Harbor Laboratory, Cold Spring Harbor, N.Y.